THE JOURNAL OF BIOLOGICAL CHEMISTRY Vol. 279, No. 40, Issue of October 1, pp. 42128–42138, 2004
Printed in U.S.A.

Speriolin Is a Novel Spermatogenic Cell-specific Centrosomal Protein Associated with the Seventh WD Motif of Cdc20*[S]

Received for publication, March 22, 2004, and in revised form, July 21, 2004
Published, JBC Papers in Press, July 26, 2004, DOI 10.1074/jbc.M403190200

Masuo Goto‡§¶ and Edward M. Eddy‡‖

From the ‡Gamete Biology Section, Laboratory of Reproductive and Developmental Toxicology, NIEHS, National Institutes of Health, Research Triangle Park, North Carolina 27709 and the §Department of Cell and Developmental Biology, University of North Carolina, Chapel Hill, North Carolina 27599

The fundamental mechanisms of mitosis are conserved throughout evolution in eukaryotes, including ubiquitin-mediated proteolysis of cell cycle regulators by the anaphase-promoting complex/cyclosome. The spindle checkpoint protein Cdc20 activates the anaphase-promoting complex/cyclosome in a substrate-specific manner. It is present in the cytoplasm and concentrated in the centrosomes throughout the cell cycle, accumulates at the kinetochores in metaphase, and is no longer detected following anaphase. However, it is unknown whether Cdc20 has the same activities and distribution during meiosis in male germ cells. We found that in mice, Cdc20 accumulates in the cytoplasm of pachytene spermatocytes during meiosis I, is distributed throughout spermatocytes undergoing meiotic division, and is present in the cytoplasm of postmeiotic spermatids. Several proteins bind to and regulate the function of Cdc20 during mitosis. We identified speriolin and determined that it is a novel spermatogenic cell-specific Cdc20-binding protein, is present in the cytoplasm, and is concentrated at the centrosomes of spermatocytes and spermatids and that a leucine zipper domain is required to target speriolin to the centrosome. The seven tandem WD motifs of Cdc20 probably fold into a seven-blade β-propeller structure, and we determined that they are required for speriolin binding and for localization of Cdc20 to the centrosomes and nucleus, suggesting that speriolin might regulate or stabilize the folding of Cdc20 during meiosis in spermatogenic cells.

The mitotic phase of the cell cycle progresses by the periodic activation and inactivation of regulatory proteins by phosphorylation and dephosphorylation (1) and by their selective destruction via the ubiquitin-proteasome pathway (2). The multiprotein anaphase-promoting complex/cyclosome (APC)[1] is the core regulatory component in this pathway (3), and a substrate-specific recruiting subunit, either Cdc20 or Cdh1, is essential for APC activation. Cdc20 is activated early in mitosis and signals the ubiquitin-mediated destruction of cyclin A, securin, and other proteins and is then degraded, whereas Cdh1 is activated during anaphase and telophase to trigger the destruction of additional substrates (2).

The location of Cdc20 in somatic cells changes during the cell cycle. In interphase, it is concentrated in the centrosomes and distributed diffusely at low levels throughout the nucleus and cytoplasm. During mitosis, Cdc20 accumulates in the nucleus in prophase, is concentrated at the kinetochores in metaphase until all chromosomes are aligned at the metaphase plate, and is no longer detected after late anaphase (4, 5). The N-terminal 167 amino acids are required for Cdc20 to associate with centrosomes (6), and this region also contains the binding domains for the spindle checkpoint protein Mad2 and the early mitotic regulator Emi1 (7–9). Mad2 competes with APC binding to the N-terminal region of Cdc20 until all kinetochores achieve bipolar attachment to the mitotic spindle, whereas Emi1 prevents Cdc20 interaction with substrates without inhibiting binding to the APC (10, 11). Dynein-dependent movement of checkpoint proteins, including Mad2, from the kinetochores along microtubules to the centrosomes occurs at the time of spindle checkpoint silencing in mitosis (12, 13), suggesting that the centrosomes contribute to this process.

The Cdc20 protein contains seven WD motifs that probably folds into a seven-blade β-propeller closed ring structure (14–16) held together by interaction of a β-strand in the first WD motif with the last of three β-strands of the seventh WD motif. When the N-terminal or C-terminal β-strand is deleted, the protein assumes a relaxed open form (17, 18). Whereas all seven of the WD motifs are required for localization of Cdc20 to the kinetochores and to the spindle apparatus (6), it is unclear how these processes occur. Furthermore, it remains to be determined how the structure of Cdc20 relates to its ability to selectively bind substrates or to its subcellular localization, including concentration at the kinetochores.

A meiotic spindle checkpoint apparently functions in mammals during spermatogenesis (19, 20) as it does during oogenesis (21, 22). Disrupting the gene for F box protein β-TrCP1, a ubiquitously expressed substrate-binding subunit of SCF ubiquitin ligase (23) reduced male fertility due to overduplication of centrosomes, formation of multipolar metaphase spindles, misaligned chromosomes, and accumulation of metaphase I spermatocytes (24). These defects were caused in part by the accumulation of Emi1 (25). The meiotic checkpoint appears to be more stringent during spermatogenesis than oogenesis, be-

* The costs of publication of this article were defrayed in part by the payment of page charges. This article must therefore be hereby marked "*advertisement*" in accordance with 18 U.S.C. Section 1734 solely to indicate this fact.

[S] The on-line version of this article (available at http://www.jbc.org) contains an additional figure.

¶ Supported in part by a long term fellowship from the TOYOBO Biotechnology Foundation (Osaka, Japan).

‖ To whom correspondence should be addressed: LRDT, C4–01, NIEHS, NIH, 111 T.W. Alexander Dr., Research Triangle Park, NC 27709. Tel.: 919-541-3015; Fax: 919-541-3800; E-mail: eddy@niehs.nih.gov.

[1] The abbreviations used are: APC, anaphase-promoting complex/cyclosome; DAPI, 4′,6-diamidino-2-phenylindole; EYFP, enhanced yellow-green fluorescent protein; GFP, green fluorescent protein; LZ, leucine zipper; mLZ, mutant LZ; 100P, 100,000 × *g* insoluble particulate fraction; PBS, phosphate-buffered saline; PBSE, PBS containing 1 mM EDTA; 100S, 100,000 × *g* soluble cytosolic fraction; contig, group of overlapping clones; GST, glutathione *S*-transferase.

This is an Open Access article under the CC BY license.

cause 10–25% of all human fetuses have an abnormal number of chromosomes due mainly (80–90%) to nondisjunction of chromosomes at maternal metaphase I (26).

These studies focused on the role of the last β-strand on the C-terminal WD motif (WD7-β4) in the subcellular localization of Cdc20 during spermatogenesis. They resulted in the identification of speriolin, a spermatogenic cell-specific protein that binds to the WD7-β4 domain of Cdc20, suggesting that it regulates Cdc20 during meiosis in male germ cells.

EXPERIMENTAL PROCEDURES

Yeast Two-hybrid Screening—Yeast two-hybrid screening was performed on ~3 million clones of a mouse testis cDNA library (Clontech) using pAS2WD7 as bait, as described previously (27). Screening, elimination of false positives, and plasmid isolation from triple positive (β-galactosidase and *His3* gene expression plus 3-amino-1,2,4-triazole resistance) clones were performed as recommended by the supplier.

Northern Blotting—A mouse Multiple Tissue Northern (MTN™) Blot (Clontech), containing 2 μg of poly(A)$^+$ RNA/lane was probed with a radiolabeled cDNA fragment. The membrane was analyzed by autoradiography at −80 °C using Kodak X-Omat AR x-ray film with an intensifying screen. The blot was exposed for 12–36 h. Blots were reused after being stripped by boiling in 0.2% SDS.

Construction of cDNA Plasmids—The cDNA fragments for fusion protein expression were prepared by PCR using *Pfu* DNA polymerase (Stratagene) or LA-*Taq* DNA polymerase (Takara) and cloned into the appropriate vectors and then verified by sequencing. For yeast two-hybrid screening, a cDNA encoding the Cdc20 N-terminal segment (amino acids 1–185) and C-terminal segment of the seven WD motif region (amino acids 442–499) was cloned into the pAS2–1 (Clontech) vector, resulting in pAS2WD7. The cDNA for wild-type or mutant Cdc20 was subcloned into pEYFP-C1 (Clontech) or pFLAG-CMV2 (Sigma) vector to add in-frame N-terminal tags.

To obtain the full-length *Sprn* cDNA, the 5′-rapid amplification of cDNA ends reaction was performed using mouse testis Marathon-Ready cDNA (Clontech) as template. The amplified fragment was cloned into pBluescript KS(+) vector and sequenced. Wild-type and mutant speriolin constructs were subcloned into pEYFP-C1 (Clontech) or pET-28a(+) (Novagen) vector to add in-frame N-terminal tags.

PCR-based random mutagenesis was performed in the presence of 0.5 mM $MnCl_2$, 1 mM dATP, 1 mM dTTP, 0.2 mM dCTP, and 0.2 mM dGTP using *Taq* DNA polymerase (Invitrogen). To produce mutations in pAS2WD7, the region encoding amino acids 442–499 of Cdc20 was replaced by randomly mutagenized cDNA fragments encoding the same region and verified by sequencing. 10 of 4,000 colonies were chosen randomly for sequencing to estimate the frequency of random mutagenesis. 8 of 10 had one or two mutations, and two were wild-type. Plasmids were extracted from four thousand transformants and pooled to produce a randomly mutagenized minilibrary (pAS2WD7mut). For speriolin (amino acids 227–480), cDNA fragments randomly mutagenized by PCR were subcloned into the pGAD10 (Clontech) vector and verified by sequencing.

Antibodies—The antibodies to speriolin were raised in rabbits against a purified His-tagged region of speriolin (amino acids 227–480), or a synthetic peptide (CRKTPHRKSNKLPDNPRDTK) corresponding to residues 309–327, conjugated via its amino-terminal cysteine was conjugated to keyhole limpet hemocyanin. Speriolin (residues 227–480) with a His_6 tag was expressed in BL21 cells, purified by nickel-nitrilotriacetic acid-agarose (Qiagen) chromatography, and further purified by extraction from a single SDS-PAGE band. The antibodies were affinity-purified by passing crude antiserum over a SulfoLink column (Pierce), to which the antigen had been coupled. Antibodies were eluted with 0.1 M glycine (pH 2.8) into tubes containing 1 M Tris-base. The pH of the pooled fractions was adjusted to neutral, and 0.1% NaN_3 was added, and the purified antisera were stored at 4 °C. The specificity of the antibodies for speriolin was determined by Western blotting using COS-7 cell lysates containing EYFP-speriolin.

Monoclonal antibody (JL-8) specific for green fluorescent protein (GFP) and enhanced yellow-green fluorescent protein (EYFP) (anti-GFP) was from Clontech. Mouse monoclonal antibodies to FLAG (M2), α-tubulin (B5-1-2), γ-tubulin (GTU-88), horseradish peroxidase-conjugated antibody to mouse IgG, and fluorescein 5-isothiocyanate-conjugated antibody to rabbit IgG were from Sigma. Alexa Fluor 546-conjugated antibody to mouse IgG was from Molecular Probes, Inc. (Eugene, OR). Antibodies to HSP70/HSC70 (BB70) and calreticulin (SPA-600) were from Stressgen. Monoclonal antibodies to p55CDC/Cdc20 (H-7) and Cdc27 (C4), rabbit polyclonal antibody to lamin B (M-20), and horseradish peroxidase-conjugated goat antibody to rabbit IgG were from Santa Cruz Biotechnology, Inc. (Santa Cruz, CA). Monoclonal antibody to pericentrin (clone 30) was from BD Transduction Laboratories.

Preparation of Mouse Tissue Extracts and Western Blotting—Various adult tissue samples from CD-1 mice were placed on ice in TN^{4}D buffer (50 mM Tris-HCl (pH 7.5), 150 mM NaCl, 50 mM NaF, 1 mM Na_3VO_4, 0.1% Nonidet P-40, 1 mM dithiothreitol, 10% glycerol, complete EDTA-free protease inhibitor tablet (Roche Applied Science)). Tissues were homogenized on ice, and then soluble and insoluble proteins were fractionated by centrifugation at 15,000 × *g* for 30 min at 4 °C. Protein concentrations were determined using a Bio-Rad protein assay kit II, and aliquots were stored at −80 °C. Whole cell extracts of fractionated germ cells or sperm were prepared by boiling cells in SDS sample buffer for 10 min. Equal loads of proteins from tissue lysates (30 μg/lane) were separated on 10% SDS-polyacrylamide gels and then electroblotted onto Immobilon membrane (Millipore Corp.). Antigen-antibody complexes were detected by ECL (Amersham Biosciences). Animal care and use were in accordance with United States Public Health Service guidelines, and procedures used in these studies involving animals were approved by the Institutional Animal Care and Use Committee of the National Institute of Environmental Health Sciences.

Cell Culture and Transient Transfection—COS-7 or BALB/3T3 cells were grown in Dulbecco's modified Eagle's medium supplemented with 10% fetal calf serum, 2 mM glutamine, 100 units/ml penicillin, and 100 μg/ml streptomycin sulfate. Cells were incubated in 5% CO_2 and 95% air at 37 °C. For transfection, plasmids were prepared with the EndoFree Plasmid Maxi Kit (Qiagen). Transient transfections were carried out with *Trans*It-LT1 (Mirus) according to the manufacturer's protocol.

For fluorescence microscopic observation, transfected cells were maintained in 2- or 4-well chamber slides (Lab-Tech) for 24 h at 37 °C. After washing with phosphate-buffered saline (PBS), cells were fixed with 4% paraformaldehyde in PBS, and then immunofluorescence staining was performed. For visualization of nuclei, cells were counterstained with 4′,6-diamidino-2-phenylindole (DAPI; Sigma).

Immunoprecipitation and Pull-down Assay—For immunoprecipitation, cells transfected with FLAG- and EYFP-tagged proteins were lysed in TN^{4}D buffer by sonication and cleared by centrifugation at 15,000 × *g* for 30 min at 4 °C. Lysates were immunoprecipitated using anti-FLAG M2 affinity gel (Sigma) in immunoprecipitation buffer (50 mM Tris-HCl (pH 7.5), 150 mM NaCl, 0.4 mM dithiothreitol, 19 mM NaF, 37 μM Na_3VO_4, 0.037% Nonidet P-40, 10% glycerol) containing freshly added protease inhibitors (complete EDTA-free protease inhibitor tablets; Roche Applied Science) for 2 h at 4 °C on a rotating platform. Immunoprecipitates were washed with PBS, boiled in SDS-sample buffer (65 mM Tris-HCl (pH 6.8), 2.5% β-mercaptoethanol, 10% glycerol, 2% SDS, 0.07% bromphenol blue), subjected to 10% SDS-PAGE, and then electrotransferred onto an Immobilon membrane.

For pull-down assay, GST-speriolin (residues 227–480) bound to glutathione-agarose (Sigma) was used as bait. GST bound to glutathione-agarose was used as negative control. Adult CD-1 mouse testis was homogenized in SDS lysis buffer (0.1% SDS, 1% Nonidet P-40, 150 mM NaCl, 0.5% deoxycholate, 50 mM Tris-HCl (pH 7.4), 10% glycerol, and protease inhibitor tablet (Roche Applied Science)). The soluble fraction was diluted to 10 times the original volume in PBS containing protease inhibitors, mixed with bait, and then rotated for 2 h at 4 °C. After washing the pellet three times with PBS, proteins were eluted using SDS sample buffer and then subjected to SDS-PAGE and Western blotting. Membrane was then stained by Coomassie Blue (Bio-Rad).

Immunostaining of Testis Sections—Immunohistochemical localization was carried out on 6-μm sections of paraffin-embedded tissue samples using a Vectastain ABC kit (Vector). The slides were incubated overnight at 4 °C with primary antibodies, diluted with automation buffer (Biomeda Corp.) containing 1% bovine serum albumin (BA-buffer), in a humidified chamber. Monoclonal antibody to Cdc20 (H-7) was diluted 1:100, and antiserum to speriolin was diluted 1:2000 with BA-buffer. Slides were stained with 3,3′-diaminobenzidine and counterstained with hematoxylin (Vector).

Immunofluorescence Staining of Isolated Germ Cells—Mixed germ cells were isolated from testes of adult CD-1 mice, with minor modifications of established procedures (28). Seminiferous tubules were dissociated in enriched Krebs-Ringer bicarbonate medium containing collagenase (0.5 mg/ml) and trypsin (0.25 mg/ml). Following filtration through 80-μm nylon mesh and centrifugation, cells were suspended in enriched Krebs-Ringer bicarbonate to a final concentration of ~10^6/ml and transferred onto a SuperFrost plus microscope slide (Fisher). Cells were fixed with 4% paraformaldehyde/PBS for 10 min, permeabilized

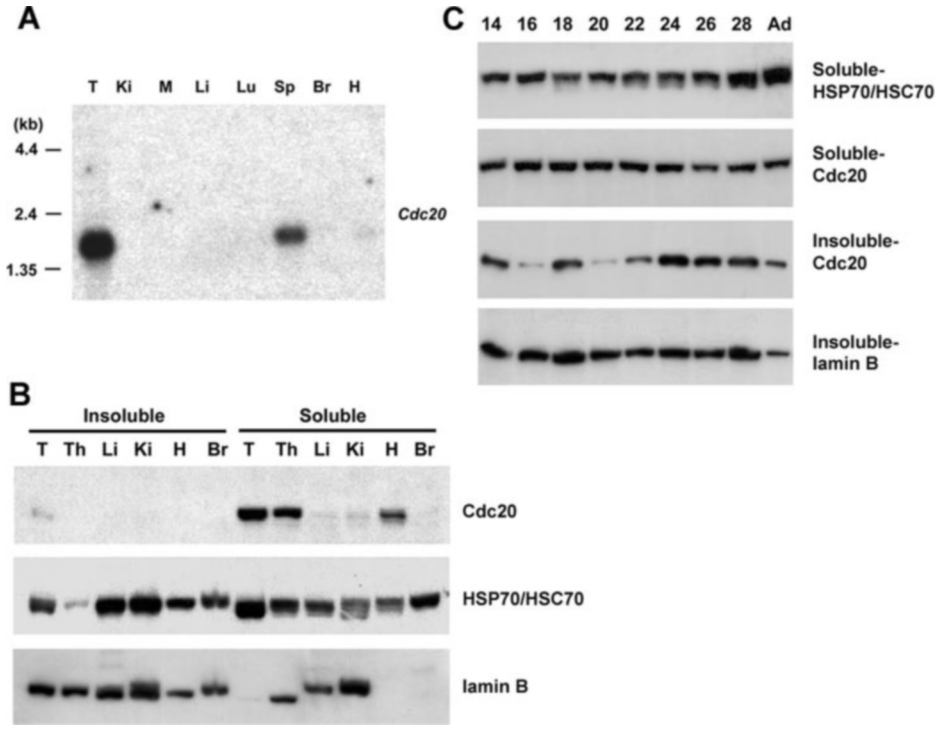

FIG. 1. **Expression of Cdc20 in testis.** *A*, Northern blot analysis of mouse tissue mRNAs. *Cdc20* mRNA is abundant in whole testis. *B*, 0.1% Nonidet P-40-soluble and -insoluble tissue extracts from adult mouse tissues were separated by 10% SDS-PAGE followed by Western blotting with a monoclonal antibody to Cdc20 (*top panel*). Antibodies to HSP70/HSC70 and lamin B were used as loading controls (*bottom two panels*). Cdc20 was detected in the testis soluble and insoluble fractions. *T*, adult testis; *Ki*, kidney; *M*, skeletal muscle; *Li*, liver; *Lu*, lung; *Sp*, spleen; *Br*, brain; *H*, heart; *Th*, thymus. *C*, Cdc20 expression in testis is regulated developmentally. Extracts were prepared from testes of wild type juvenile mice on postnatal days 14, 16, 18, 20, 22, 24, 26, and 28 and from testes of adult (*Ad*) mice, as indicated. 0.1% Nonidet P-40-soluble (*upper two panels*) and -insoluble (*lower two panels*) tissue extracts were subjected to Western blotting for the proteins indicated on the *right*.

with 0.5% Triton X-100 for 5 min at 4 °C, and then blocked with 5% normal goat serum in BA-buffer. Cells were labeled for 2 h at room temperature with primary antibodies followed by fluorescein 5-isothiocyanate-conjugated or Alexa-Fluor 546-conjugated secondary antibodies in a humidified chamber. Nuclei were labeled with DAPI, and slides were mounted with Vectashield (Vector). Protein localization was determined at a magnification of 400× using a Zeiss Axioplan fluorescence microscope and a SPOT digital camera (Diagnostic Instruments, Inc.). Final images were prepared using Adobe Photoshop Version 6.

Fractionation of Cell Lysates and Trypsin Protection Assay—Transiently transfected COS-7 cells were lysed and homogenized using a Potter-type homogenizer in Buffer A (50 mM Tris-HCl (pH 8), 0.32 M sucrose, 1 mM EDTA, 1 mM β-mercaptoethanol, complete EDTA-free protease inhibitor tablet (Roche Applied Science)) and then centrifuged at 14,000 × *g* for 30 min. The resulting supernatant was further centrifuged at 100,000 × *g* for 1 h to separate the soluble cytosolic fraction (100S) from the insoluble particulate fraction (100P). The 100P pellet was suspended in TN^4D containing 1% Nonidet P-40 and 0.5 M NaCl or in PBS containing 1 mM EDTA (PBSE) for Western blotting or trypsin protection assays, respectively. Equal amounts of protein were analyzed by Western blotting.

Four microliters of the 100P pellet obtained from lysates of COS-7 cells expressing EYFP-speriolin were resuspended in PBSE and mixed with 1 μl of 0.25% trypsin-EDTA (Invitrogen) or PBSE and incubated at 37 °C for 5 or 10 min. The reaction was stopped by adding 5 μl of 2× SDS sample buffer. Reaction mixtures were analyzed by Western blotting.

RESULTS

Presence of Cdc20 in Spermatogenic Cells—Northern and Western blotting of gels loaded with equal amounts of materials determined that Cdc20 mRNA (Fig. 1*A*) and protein (Fig. 1*B*) are abundant in the adult mouse testis and that Cdc20 protein is detected in the 0.1% Nonidet P-40-insoluble fraction of the tissue examined only in testis. The first wave of spermatogenesis in postnatal mice is relatively synchronous. The insoluble form slightly increased in amount on postnatal day 18, corresponding to the first wave of meiotic divisions, and again on postnatal day 24, when condensing spermatids are first observed (Fig. 1*C*). Although this suggested that Cdc20 is present in spermatids, it was undetectable in sperm isolated from the cauda epididymis (data not shown). The presence of Cdc20 in spermatogenic cells was confirmed by immunohistochemistry on sections of adult mouse testis. The protein was present at low levels in spermatogonia, detected at higher levels throughout the cytoplasm of midpachytene spermatocytes, and localized at the periphery of the nucleus of late pachytene spermatocytes. The Cdc20 protein was seen throughout the cytoplasm of spermatids during most of the postmeiotic phase of spermatogenesis but not in early elongating spermatids (Fig. 2). The presence of Cdc20 in spermatids was unanticipated, because in somatic cells it peaks in abundance at the G_2/M phase and disappears in late mitosis (29).

Molecular Cloning of Speriolin—Because Cdc20-binding proteins regulate its function during mitosis, we hypothesized that novel proteins might be involved in regulating Cdc20 function during meiosis in spermatogenic cells. To identify a Cdc20-binding protein, a mouse testis library was screened using the yeast two-hybrid method. Screening with the full-length Cdc20 protein resulted in a large number of false positives. Therefore, a bait vector (pAS2WD7) was constructed with a cDNA encoding the N-terminal 185 amino acids (containing WD1-β1) and the C-terminal 57 amino acids (containing WD7-β2, -β3, and -β4) of Cdc20 that was expected to express a WD motif with four β strands as a GAL4-BP fusion protein (Cdc20-WD). Empty vector was used as a control. This led to the isolation of three clones, and sequencing determined that their cDNA inserts varied in length but encoded the same protein. A full-length cDNA was assembled from the overlapping sequences of the original clones (nucleotides 109–1607), and a fragment was generated using the 5′-rapid amplification of cDNA ends pro-

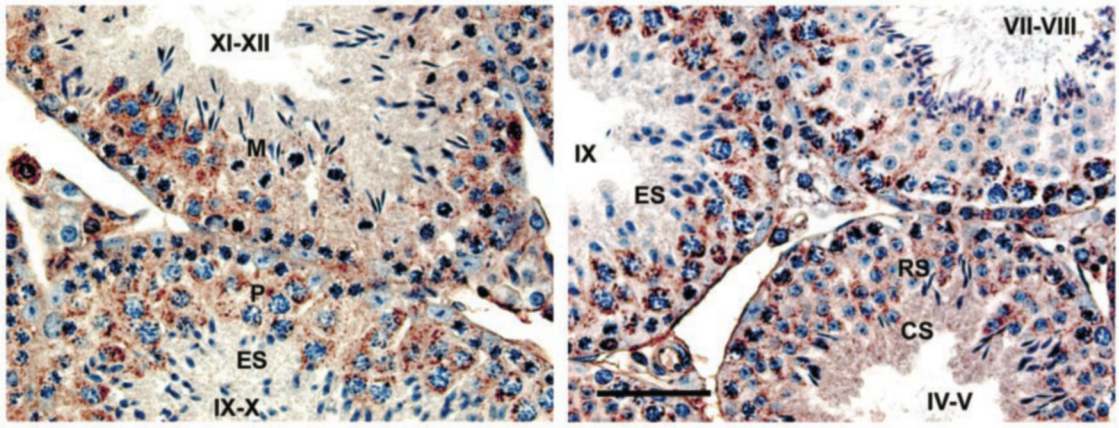

FIG. 2. **Immunohistochemical localization of Cdc20 in sections of adult mouse testis.** Sections of adult mouse testis were immunostained with monoclonal antibody to Cdc20. Cdc20 was most abundant in the cytoplasm of pachytene spermatocytes (*P*). Immunostaining was also detected in spermatocytes undergoing meiotic division (*M*) and in round (*RS*) and condensing (*CS*) spermatids while undetectable in early elongating spermatids (*ES*). Stages of spermatogenesis are indicated in *Roman numerals*. *Bar*, 50 μm.

cedure (nucleotides 1–630). An open reading frame between nucleotides 72 and 1514 encoded a novel protein containing 480 amino acids with a leucine zipper (LZ) motif at the N terminus (amino acids 3–37), a calculated molecular mass of 51,400 daltons, and a predicted pI of 8.16. We named the protein speriolin (SPRN). We confirmed physical interaction between speriolin and Cdc20 by pull-down assays using testis lysates (Fig. 3). We also found that speriolin co-precipitated Cdc27 (Fig. 3), a component of APC, together with Cdc20, suggesting that speriolin binds to APC^{Cdc20} in testis. Data base searching determined that an uncharacterized sequence in GenBank™ is identical to nucleotides 14–1592 of the *Sprn* cDNA (accession number AK006994; RIKEN clone 1700084J23, *Mus musculus* adult male testis). It also was determined that the *Sprn* gene is located within the WGS supercontig Mm15_WIFeb01_286 (genomic contig: NW_000106) and spans a region of ~23.8 kb located on mouse chromosome 15D3 that is syntenic with human chromosome 8q24. The gene contains five exons, and the proposed exon-intron boundaries follow the canonical GT/AG rule (data not shown). The *Sprn* cDNA sequence was deposited in GenBank™ (accession number AB032199). A scan of the NCBI mouse genome data base using BLAST did not detect any *Sprn* pseudogenes.

Speriolin Expression and Localization—Northern analysis determined that among the mouse tissues examined, the *Sprn* message is specific to the testis (Fig. 4*A*). Speriolin protein also was detected only in testis homogenates by Western blotting using either affinity-purified rabbit antisera to His_6-tagged fusion protein (amino acids 227–480) (Fig. 4*B*) or to a synthetic peptide (amino acids 309–327) (data not shown). The preimmune serum (data not shown) and the antisera preabsorbed with His-tagged speriolin were negative on testis (Fig. 4*B*), providing evidence that the antisera are specific to endogenous speriolin. Whereas Cdc20 was found primarily in the 0.1% Nonidet P-40-soluble fraction and in limited amounts in the insoluble fraction of testis homogenates by Western blotting, speriolin was detected only in the insoluble fraction (Fig. 4*C*). Western blotting of developmental stages of testis further indicated that expression of speriolin begins between days 14 and 16, when pachytene spermatocytes develop, increases by day 22, when postmeiotic spermatids are seen, and is abundant in epididymal sperm but is not detected in adult ovary (Fig. 4*D*). These observations were consistent with the immunohistochemical analysis. Speriolin is first seen in late pachytene spermatocytes, is abundant throughout spermatocytes undergoing meiotic division, and is present in the cytoplasm of spermatids (Fig. 5).

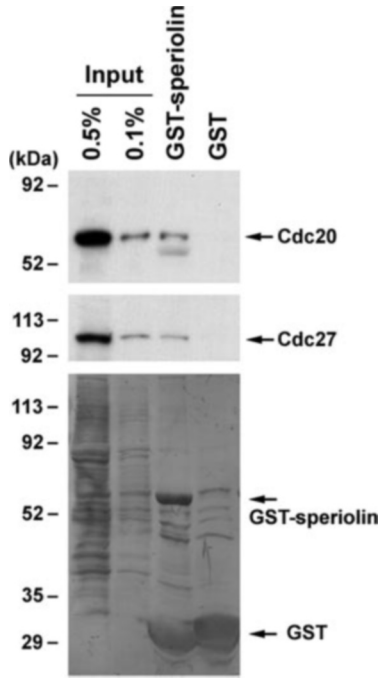

FIG. 3. **Cdc20 associates with speriolin.** Pull-down experiments of testis lysate were carried out with GST-speriolin (amino acids 227–480). GST was used as control. Cdc20 and Cdc27 were detected by Western blotting (*upper two panels*) followed by Coomassie Blue staining (*bottom panel*). A band slightly smaller than Cdc20 (about 53 kDa in the *upper panel*) was a nonspecific signal derived from GST-speriolin.

Immunofluorescence assays on mixed spermatogenic cells isolated from adult mouse testis were used to determine the subcellular distribution of speriolin (Fig. 6). The cytoplasm was weakly stained, but one or two spots in the cytoplasm were more intensely stained in pachytene spermatocytes, spermatocytes undergoing meiotic division, round spermatids, and condensed spermatids, suggesting that speriolin accumulates in the centrosome. This was confirmed by immunostaining of isolated germ cells simultaneously with antibodies to speriolin and to the centrosomal protein pericentrin and determining that the two proteins are co-localized in spermatocytes (Fig. 6). We also confirmed that pericentrin is undetectable in spermatids (30) but found that speriolin was localized to the centrosomes in these cells. These results strongly suggest that speriolin is a spermatogenic cell-specific centrosomal protein.

The Leucine Zipper Motif Is Required for Localization of Speriolin to the Centrosome—A series of EYFP-speriolin dele-

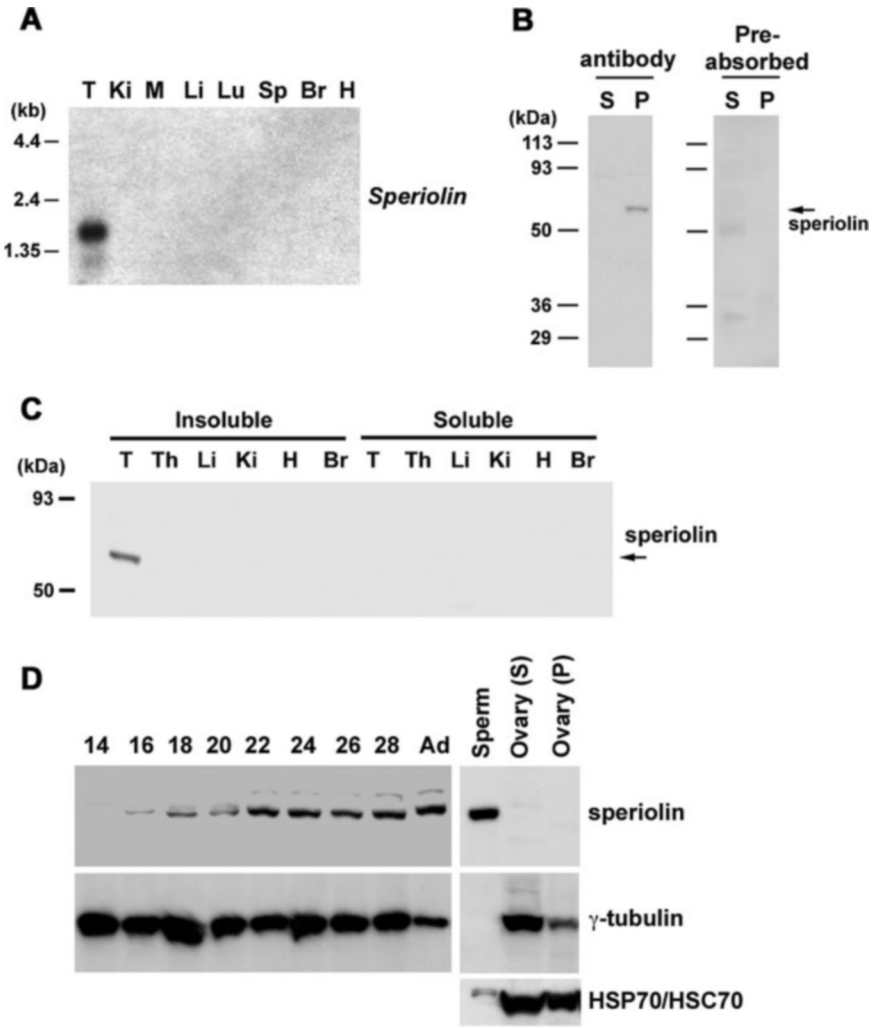

FIG. 4. **Expression of speriolin in testis.** *A*, speriolin mRNA was detected only in testis. Mouse tissue mRNA blot used in Fig. 1*A* was probed with speriolin cDNA. *B*, antibody to speriolin detected a 53-kDa band in the 0.1% Nonidet P-40-insoluble fraction (*P*) of testis lysate, whereas speriolin was undetectable in the soluble fraction (*S*) of testis lysate. Speriolin was undetectable in testis lysates using antibody that was preabsorbed by His-tagged speriolin (*right panel*). *C*, 0.1% Nonidet P-40-soluble and -insoluble tissue extracts from adult mouse tissues, as indicated in Fig. 1*B*, were probed with an affinity-purified antiserum to speriolin. A 53-kDa band was specifically detected in the testis-insoluble fraction. *D*, speriolin expression is developmentally regulated in testis and abundant in epididymal sperm. Extracts were prepared from testes of wild type mice at postnatal day 14, 16, 18, 20, 22, 24, 26, and 28, adult (*Ad*) testes, sperm from cauda epididymis, and soluble (*S*) and insoluble (*P*) fractions from adult mouse ovary, as indicated. 0.1% Nonidet P-40-insoluble tissue extracts were subjected to Western blotting with antiserum to speriolin (*top panel*). Immunostaining for γ-tubulin (*lower panel*) was used as a loading control for testis extracts and negative control for epididymal sperm extracts, respectively. Immunostaining for HSP70/HSC70 was used as a loading control for sperm and ovary extracts.

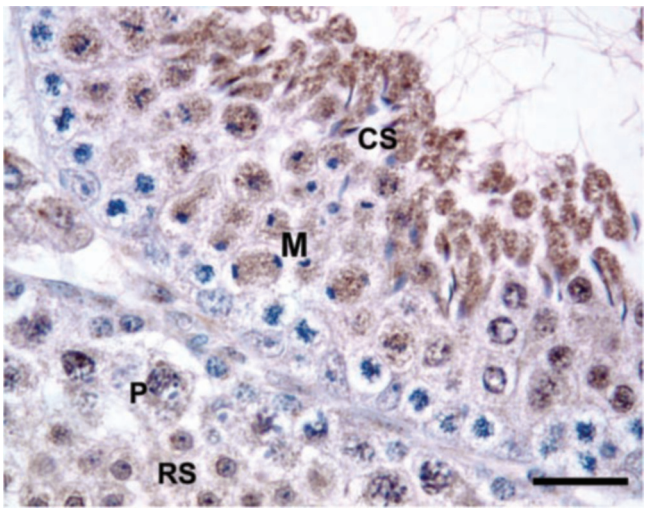

FIG. 5. **Immunohistochemical localization of speriolin in testis.** Histological sections of Bouin's fixed and paraffin-embedded adult mouse testis were incubated with affinity-purified antibody to speriolin. Speriolin was detected in spermatocytes undergoing meiotic division (*M*). Staining was detected in pachytene spermatocytes (*P*) and round spermatids (*RS*) and was abundant in the cytoplasm of condensing spermatids (*CS*). *Bar*, 25 μm.

tion mutants were generated to identify the domain responsible for centrosomal targeting. Recombinant EYFP-speriolin expressed in BALB/3T3 cells following transient transfection was localized in one or two spots in the cytoplasm immediately adjacent to the nucleus (Fig. 7*A*). This localization was comparable with the subcellular distribution of endogenous speriolin in spermatogenic cells (Fig. 6), demonstrating that this heterologous cell system could be utilized for analysis of speriolin localization. Speriolin deletion mutant N76, expressing only the N-terminal 76 amino acids of speriolin containing the LZ domain, was localized adjacent to the nucleus in one or more spots that varied in size between cells, probably due to different levels of expression. This suggests that the N-terminal leucine zipper domain has a key role in targeting speriolin to the centrosome. However, speriolin deletion mutant ΔD, lacking 28 amino acids (residues 426–454) from the C-terminal region that contains two D-box-like domains (R*XX*L), was distributed in a reticular pattern throughout the cytoplasm. Additional studies will be needed to determine whether this region is involved directly in centrosomal localization or if the pattern seen was caused by a change in speriolin conformation due to the deletion. Speriolin mutant mLZ, in which valines were substituted for Leu-10, Leu-17, and Leu-24 in the LZ domain, was located in multiple perinuclear spots (Fig. 7, *A* and *B*). Treating cells with brefeldin A did not alter the distribution of mLZ, indicating that it was unlikely to be accumulating in the Golgi apparatus (data not shown). The result with mutant mLZ provides further evidence that the leucine zipper domain is involved in targeting speriolin to the centrosome.

Full-length speriolin and deletion mutant N76 colocalized with the centrosomal protein pericentrin, confirming their association with the centrosome. An unexpected finding was that pericentrin colocalized in multiple perinuclear spots with spe-

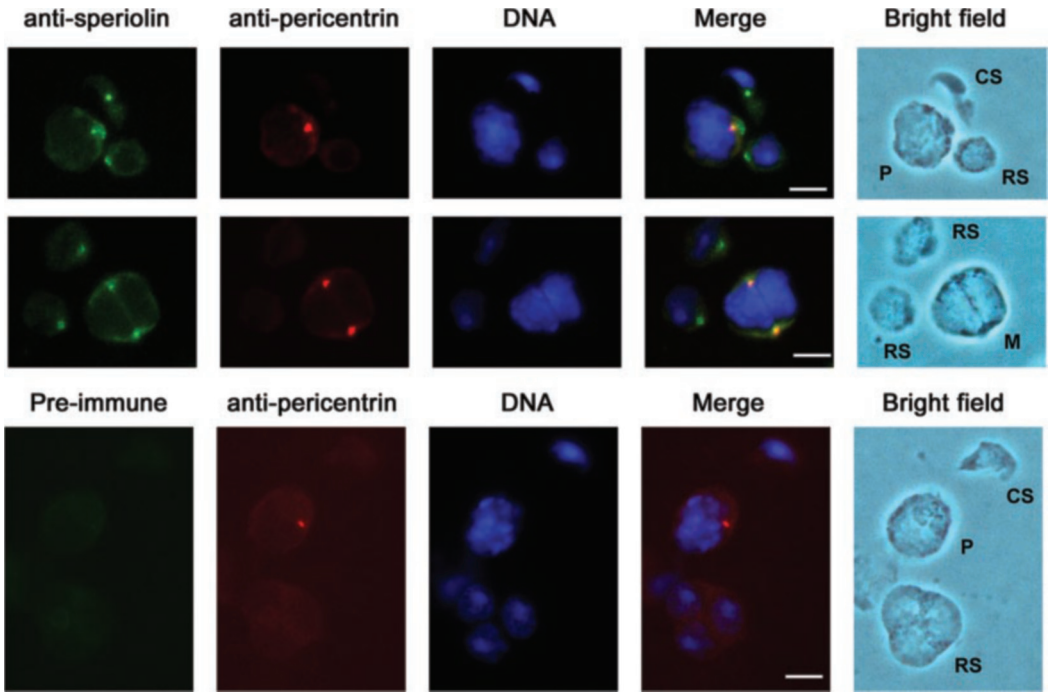

FIG. 6. **Speriolin is localized at centrosomes in spermatogenic cells.** Spermatogenic cells isolated from adult mice were fixed on slides and stained with speriolin (*green*) and pericentrin (*red*) antibodies and DAPI (*blue*). Preimmune serum was used as a negative control (*bottom panel*). Speriolin and pericentrin were co-localized in pachytene spermatocytes (*P*) and in cells undergoing meiotic division (*M*), as indicated by the *yellow signal*. Round (*RS*) or condensing (*CS*) spermatids were stained only by speriolin (*green dots*). *Bar*, 10 μm.

riolin mutant mLZ, suggesting that the association between speriolin and pericentrin is LZ domain-independent. However, the amount of pericentrin appeared to increase in the presence of mLZ (Fig. 7*A*), suggesting that the speriolin LZ domain is involved in pericentrin turnover. As controls for these experiments, an antibody to α-tubulin was used to verify that the cytoskeleton was not disrupted by the expression of either EYFP alone or the EYFP-tagged mutant speriolin proteins (Fig. 7*B*). In addition, Western blotting with an antibody to GFP verified that the mutant speriolin proteins were intact (data not shown).

Subcellular Distribution of Speriolin—We examined the distribution of EYFP-speriolin in cell fractions separated by differential centrifugation to determine its association with other cellular components. The low speed supernatant (12,000 $\times$ *g*) of homogenates of COS-7 cells expressing full-length and deletion mutants of EYFP-speriolin were further separated by centrifugation at high speed (100,000 $\times$ *g*) into cytosolic (100S) and microsomal fractions (100P). When equal amounts of protein from each fraction were subjected to SDS-PAGE and Western blotting, EYFP-speriolin was detected mainly in the 100P fraction, whereas EYFP-speriolin deletion mutant ΔD was present in both fractions (Fig. 7*C*). Because the centrosome is a nonmembranous organelle, we investigated the membrane topology of EYFP-speriolin in the 100P fraction by limited trypsin-digestion analysis. As a control, we monitored endogenous calreticulin, one of the major Ca^{2+}-binding proteins present in the lumen of the endoplasmic reticulum. A level of trypsin digestion that did not affect calreticulin was determined by Western blotting with an antibody to calreticulin. Under the same conditions, EYFP-speriolin and EYFP-speriolin deletion mutant ΔD in the P100 fraction were trypsin-sensitive, consistent with speriolin being at the cytoplasmic face of a nonmembranous component of the particulate fraction, such as the centrosome (Fig. 7*D*).

The localization of speriolin in the centrosome suggested that it might associate with other centrosomal proteins. We used co-precipitation assays to examine the association between FLAG-speriolin and EYFP-tagged γ-tubulin, ODF1, or ODF2 co-expressed in COS-7 cells. FLAG-speriolin bound to EYFP-tagged γ-tubulin (Fig. 8*A*), but not to ODF1 or ODF2 (data not shown). The amounts of EYFP-γ-tubulin that co-precipitated with full-length (amino acids 1–480) or the C-terminal half (amino acids 285–480) of speriolin appeared to be less than what co-precipitated with the other speriolin deletion mutants (containing amino acids 70–480 or 161–480). This suggests that the region of speriolin containing amino acids 161–284 participates in the interaction with γ-tubulin and that the LZ domain of speriolin interferes with γ-tubulin association. We also confirmed that γ-tubulin was recovered as a complex with GST-speriolin from testis lysate by pull-down experiments (Fig. 8*B*). However, it remains to be determined whether the association between γ-tubulin with speriolin is direct or indirect.

The Cdc20-binding Domain on Speriolin—Yeast two-hybrid analysis using Cdc20-WD and N-terminal and C-terminal deletion mutants of speriolin determined that the C-terminal region of speriolin containing amino acids 283–480 is required for Cdc20 binding (Fig. 9*A*). This region was dissected further using Cdc20 as bait to screen a yeast two-hybrid minilibrary constructed following introduction of random mutations into the cDNA encoding the C-terminal half of speriolin. Fourteen clones were isolated that lacked binding activity, 11 of which had nonsense mutations and three of which had single or double amino acid substitutions. All three substitutions (V305M, K302R/R314Q, and L469P) were located near the ends of the Cdc20-binding region (Fig. 9*A*, *diamonds*). This region contained no previously identified protein-protein binding sequences, suggesting that speriolin-Cdc20 binding is dependent on secondary structure or on novel binding sequences.

Further analysis of the physical interaction between speriolin and Cdc20 was carried out using co-immunoprecipitation assays. A series of FLAG-speriolin mutants were co-expressed with EYFP-Cdc20 in COS-7 cells. EYFP-Cdc20 was co-immu-

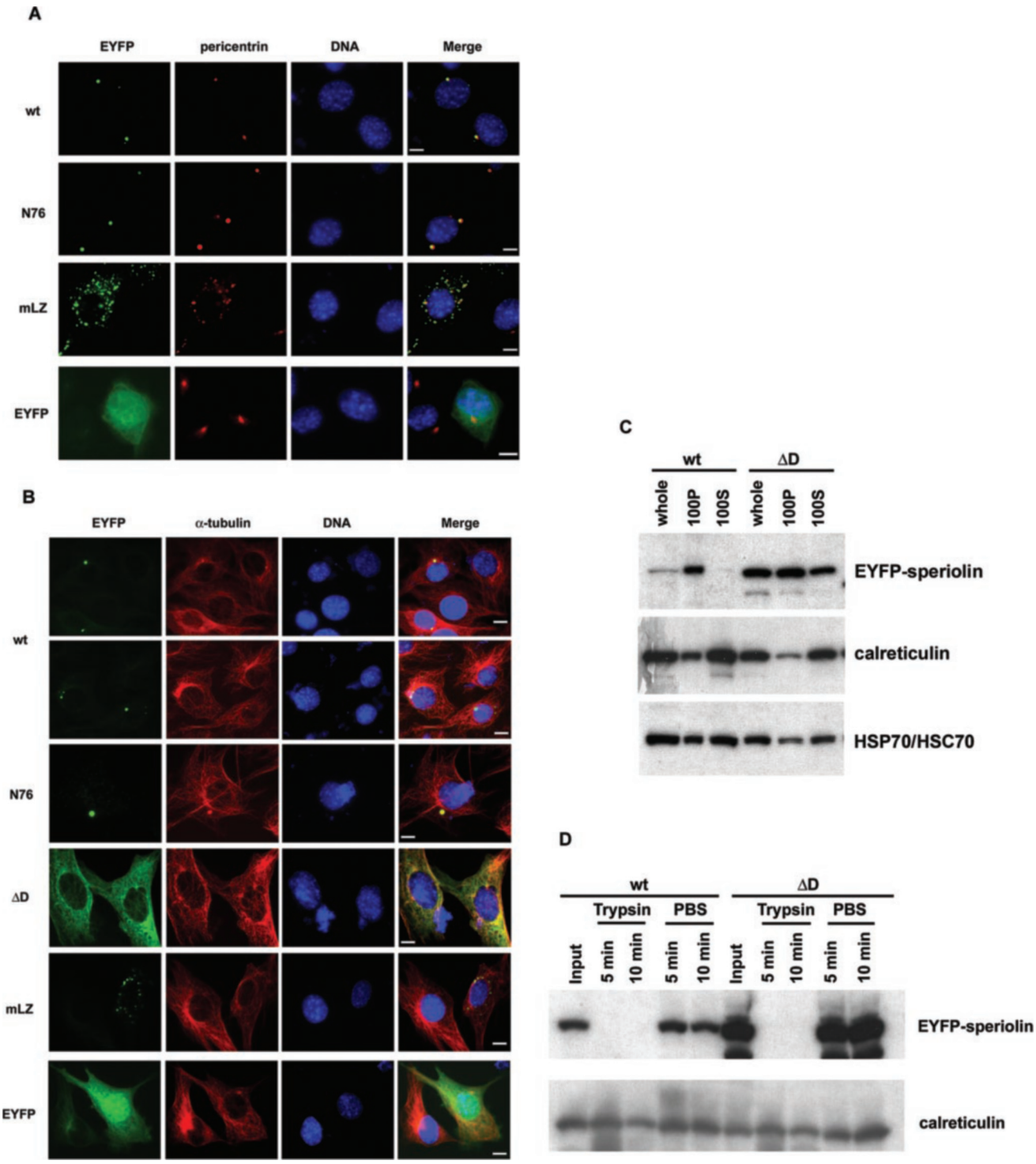

FIG. 7. **Subcellular localization of EYFP-speriolin in BALB/3T3 cells.** *A*, centrosomal localization of EYFP-speriolin in BALB/3T3 cells. Vectors containing full-length *Sprn* cDNA (*wt*), the N-terminal 76 amino acids (*N76*), and a disrupted leucine zipper (*mLZ*) were transiently transfected into BALB/3T3 cells. Cells were fixed and stained with monoclonal antibody to pericentrin followed by the Alexa 546-labeled anti-mouse IgG and DAPI (*blue*). The subcellular localization of EYFP (*bright yellow-green*) and pericentrin (*red*) were viewed by fluorescence microscopy. Co-localized signals appear in *yellow*. Empty vector was used as control (*EYFP*). *Bar*, 10 μm. *B*, cDNAs for full-length *Sprn* (*wt*) or mutants with a deletion (amino acids 426–454) in the C-terminal region containing the D-box-like sequence (Δ*D*), containing only the N-terminal 76 amino acids (*N76*), or with a disrupted leucine zipper (*mLZ*) were inserted into the mammalian expression vector pEYFP-C1 (*EYFP*). Transiently transfected BALB/3T3 cells were fixed and stained with monoclonal antibody to α-tubulin followed by the Alexa Fluor 546-labeled anti-mouse IgG and DAPI (*blue*) for DNA. The subcellular localization of EYFP (*bright yellow-green*) and α-tubulin (*red*) were viewed by fluorescence microscopy. *C*, distribution of EYFP-speriolin in fractions of transiently transfected COS-7 cells. Cells were harvested, disrupted using a Potter-type homogenizer, and then centrifuged at 12,000 × *g* for 10 min to remove nuclei and mitochondria. The resulting supernatant was further centrifuged at 100,000 × *g* for 1 h to separate the soluble cytosolic fraction (100S) from the insoluble particulate fraction (100P). Aliquots of fractionated or unfractionated cell extracts (whole) were subjected to 10% SDS-PAGE and analyzed by Western blotting with monoclonal antibodies to GFP, HSP70/HSC70 (a protein loading control), or antiserum to calreticulin (an endoplasmic reticulum-resident protein) as indicated. *D*, limited trypsin digestion assay on EYFP-speriolin in fractions of transiently transfected COS-7 cells. Aliquots of the isolated particulate fraction (100P) were treated with either 0.05% trypsin or PBS containing 1 mM EDTA for 5 or 10 min followed by 10% SDS-PAGE. Western blotting was performed using antibodies to GFP (*upper panel*) and calreticulin (*lower panel*). Untreated 100P fraction was used as a positive control (*Input*). These results show that speriolin is exposed on the surface of a particulate component.

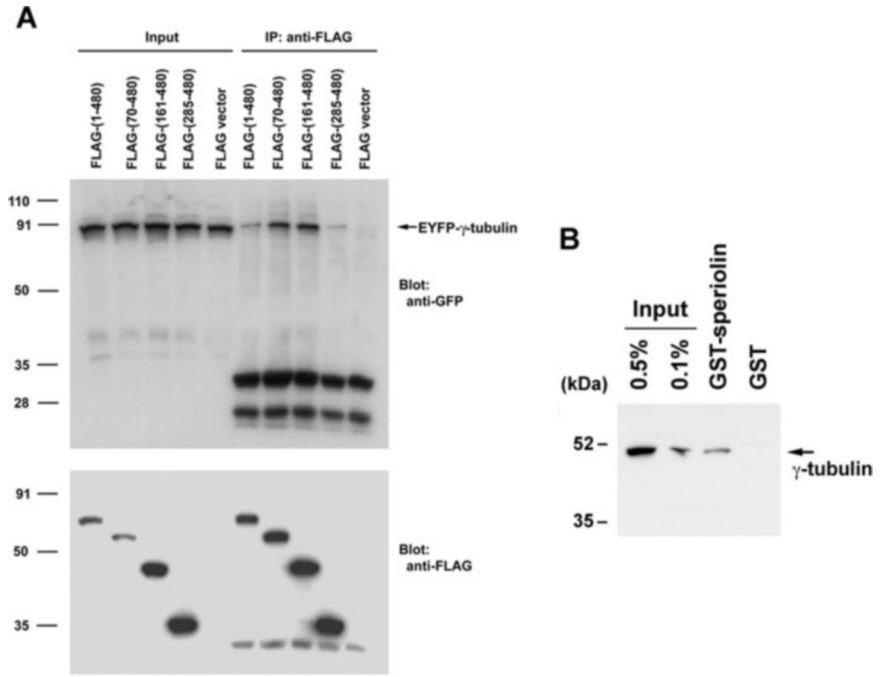

FIG. 8. **Association of speriolin with γ-tubulin.** *A*, participation of middle region of speriolin in association with γ-tubulin. FLAG-tagged speriolin was recovered from lysates of COS-7 cells co-expressing EYFP-γ-tubulin and FLAG-tagged mutant speriolin using anti-FLAG affinity gel. Immunoprecipitants were separated by SDS-PAGE and subjected to Western blotting using antibodies to GFP for detection of EYFP-γ-tubulin (*upper panel*) or FLAG (*lower panel*). Empty vector (FLAG vector) was used as negative control. *B*, recovery of γ-tubulin from testis lysates as a complex with GST-speriolin. Pull-down experiments of testis lysate were carried out as shown in Fig. 3. Stripped membrane was reprobed with monoclonal antibody to γ-tubulin.

noprecipitated with FLAG-speriolin but not with C-terminal truncated FLAG-speriolin or FLAG alone (Fig. 9*B*), providing additional evidence that Cdc20 binds to a region in the C-terminal half of speriolin.

The Speriolin-binding Domain on Cdc20—The WD7-β4 region is critical for folding of other β-propeller proteins (17, 18) and was included in the Cdc20 bait used to screen the yeast two-hybrid library, leading us to hypothesize that this region of Cdc20 is required for binding to speriolin. This was tested by introducing random mutations into the WD7-β2, -β3, and -β4 domains of Cdc20. When 35 negative clones (no speriolin binding) and 15 positive clones were sequenced, 31 of the negative clones had nonsense mutations between β2 and β3, whereas the other four contained point mutations in WD7-β4 that were predicted to disrupt the β4 structure (E465V, R468Q, E474K, and P477T). In contrast, none of the positive clones that bound to speriolin had mutations that disrupted the β4 structure (R471L). One of the negative clones contained a mutation that altered the length of the β4 structure (E465V), suggesting that this also has a critical role for Cdc20 binding (Fig. 9*C*).

We used co-immunoprecipitation-Western assays to confirm the association between speriolin and Cdc20. Cell lysates were prepared from COS-7 cells co-expressing FLAG-speriolin and EYFP-tagged mouse Cdc20, p55Cdc (rat ortholog of Cdc20), or Cdc20 with mutations disrupting the WD7-β4 structure (R468Q/W470G or truncated at amino acid 457). Mouse EYFP-Cdc20 and rat EYFP-p55Cdc were co-precipitated with FLAG-speriolin, but EYFP-tagged mutant Cdc20 or EYFP alone were not (Fig. 9*D*). This was consistent with the yeast two-hybrid results (Fig. 9*C*) and confirmed that physical interaction occurs between speriolin and Cdc20.

Intracellular Localization of Intact and Mutated Cdc20—Deletion of either the N-terminal or C-terminal β-strands of WD motifs cause other β-propeller proteins to assume a relaxed open form (17, 18). In addition, the WD repeats are required for Cdc20 localization to kinetochores (6). This suggests that Cdc20 is present in the relaxed open form when it accumulates in the cytoplasm of late pachytene spermatocytes. To examine this possibility, EYFP-tagged Cdc20 that either was intact, had point mutations in WD7-β4 (R468Q and W470G), or had WD7-β4 deleted (Δ465–474) was expressed in COS-7 cells. Intact Cdc20 was associated with kinetochores in the nucleus of some cells (Fig. 10*A*, *wt*) and distributed in the cytoplasm of others (data not shown), consistent with previous reports of variation in the location of Cdc20 during different stages of the cell cycle (5, 6). In contrast, Cdc20 with the point mutations or with WD7-β4 deleted failed to localize to the nucleus and accumulated in a reticular pattern in the cytoplasm (Fig. 10*A*). Brefeldin A treatment did not alter the pattern of distribution (data not shown). Controls demonstrated that EYFP alone was located predominantly in the nucleus (data not shown) and confirmed that the mutated proteins were expressed intact (Fig. 10*B*).

DISCUSSION

These studies focused on Cdc20 as an approach to gaining a better understanding of the regulation of meiosis in spermatogenic cells. In the mitotic cell cycle, Cdc20 is present at low levels throughout the nucleus and cytoplasm, is abundant in the centrosomes during interphase, accumulates in the nucleus during prophase, and is concentrated at the kinetochores from late prophase until late anaphase (4–6, 10). During exit from mitosis, Cdc20 is replaced by Cdh1 and is degraded by APC^{Cdh1}, which remains active throughout the G_1 phase (2). We found that Cdc20 accumulates in the cytoplasm of late pachytene spermatocytes during prophase of meiosis I and is present in cells undergoing meiotic division, similar to what occurs during mitosis. This pattern of expression suggests that Cdc20 serves similar purposes during mitosis and meiosis. An unexpected finding in these studies was that Cdc20 is not absent after the meiotic divisions but is present in round spermatids, not seen in early elongating spermatids, and becomes abundant again in late elongating spermatids. However, Cdc20 and the APC are suggested to have other roles in addition to regulation of mitosis (2, 29, 32). Recent studies indicate that the APC^{Cdh1} might function outside the cell cycle, both in the degradation of a regulator of transforming growth factor β signaling (29) and in postmitotic neurons (33). This would be consistent with Cdc20 having a novel role during the postmeiotic phase of spermatogenesis in the development or function of spermatids.

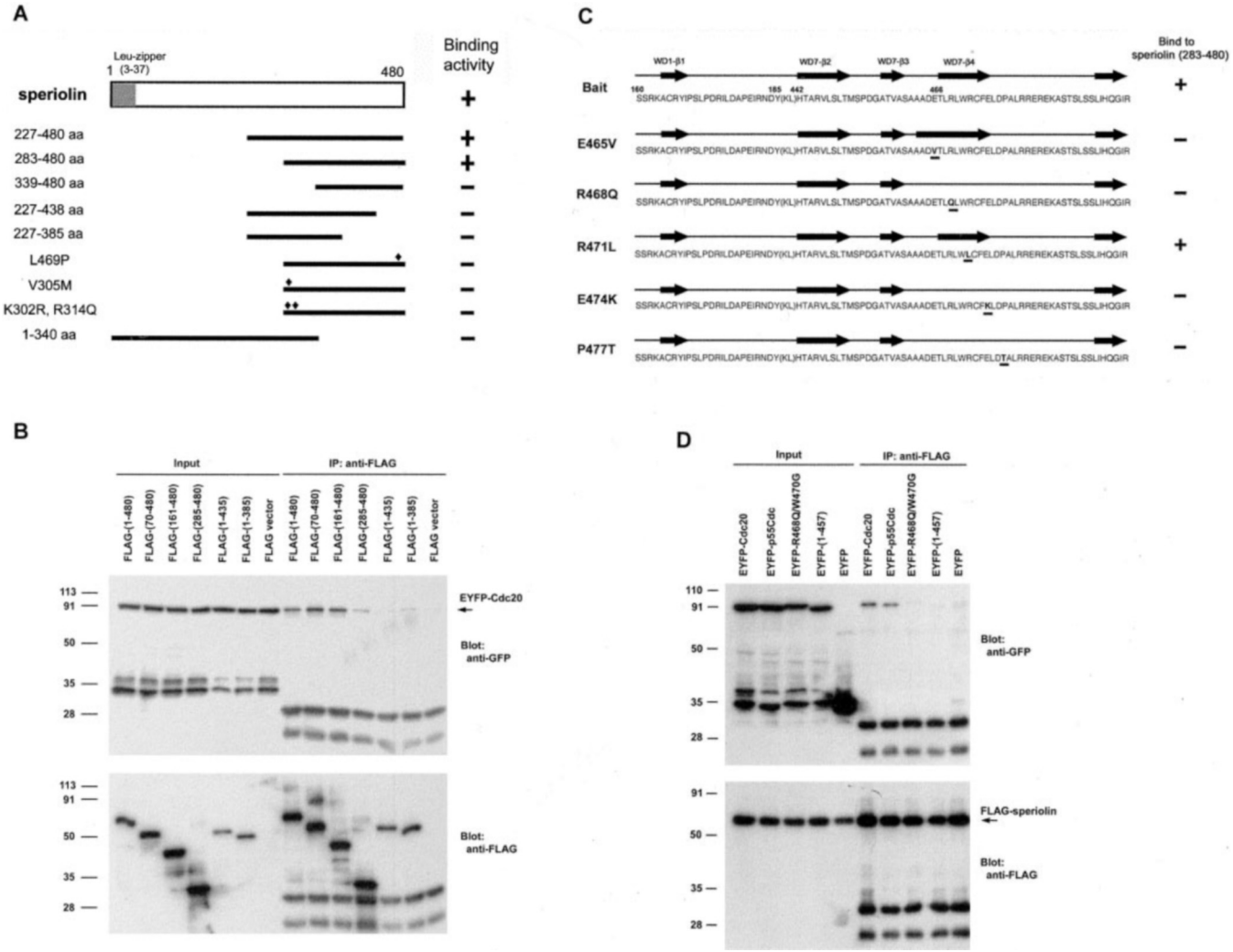

FIG. 9. **Speriolin binds to C-terminal WD motif of Cdc20.** Mouse *Speriolin* cDNA was isolated in a yeast two-hybrid screen of a mouse testis-cDNA library using Cdc20 amino acids 1–185 linked to Cdc20 amino acids 442–499 as bait. *A*, schematic representation of interactions between Cdc20 and different speriolin mutants. A leucine zipper is present at residues 3–37 of speriolin. Binding (+) or lack of binding (−) to Cdc20 are indicated. The *diamonds* indicate the position of amino acid substitutions. Empty vector was used as a control. *B*, speriolin binds to Cdc20 *in vitro*. FLAG-tagged speriolin was recovered from lysates of COS-7 cells co-expressing EYFP-Cdc20 and FLAG-tagged mutant speriolin using anti-FLAG affinity gel. Immunoprecipitants were separated by SDS-PAGE and subjected to Western blotting using antibodies to GFP for detection of EYFP-Cdc20 (*upper panel*) or FLAG (*lower panel*). Empty vector (FLAG vector) was used as a negative control. *C*, Cdc20 in which β-strand 4 of the C-terminal WD motif (*WD7-β4*) was disrupted lost the ability to bind to speriolin. The cDNA for speriolin (residues 283–480) was fused to GAL4-AD, whereas cDNA for Cdc20 was fused to GAL4-BD using the pAS2–1 vector, resulting in pAS2WD7 (*Bait*). The four predicted β strands (WD1-β1 and WD7-β2, -β3, and -β4) of the seventh propeller motif (shown in Supplemental Fig. S1) are indicated by the *arrows*. Substituted residues are *underlined* and indicated at the *left*. The relative binding activities of bait to speriolin (residues 283–480) are shown as either + or −. *D*, the WD7-β4 of Cdc20 is required for binding to speriolin. FLAG-tagged speriolin was recovered from COS-7 lysates co-expressing FLAG-speriolin with EYFP-tagged mutant Cdc20 using anti-FLAG affinity gel. Immunoprecipitants were analyzed as in *B*.

Multiple proteins have been identified that are involved in regulating Cdc20 substrate binding and APC activation during mitosis (7–9, 34). In addition, Cdc20/FZY is present in high molecular weight multiprotein complexes both in association with and separate from the APC in HeLa cells (31) and *Xenopus* egg extracts (9, 35), suggesting that other Cdc20-interacting proteins remain to be identified. We also found that Cdc20 is associated with 0.1% Nonidet P-40-insoluble proteins in testis extracts, whereas it is present in the soluble fraction of tissue culture cells (4). These observations encouraged us to use yeast two-hybrid screening to determine whether meiosis-specific Cdc20-binding proteins are present in spermatogenic cells. This led to the identification of speriolin, a novel testis-specific protein that co-expresses with Cdc20, localizes to centrosomes in spermatocytes and spermatids, and co-localizes with pericentrin in pachytene spermatocytes. In addition, FLAG-speriolin co-precipitates from COS-7 lysates with γ-tubulin, and EYFP-tagged speriolin co-localizes with pericentrin when transfected into BALB/3T3 cells. Mutational analysis showed that the C-terminal region of speriolin is required for Cdc20 binding and that the N-terminal LZ domain is required for speriolin to accumulate in centrosomes, but not for pericentrin to co-localize with speriolin or for γ-tubulin to co-precipitate with speriolin. The ability of speriolin to bind to Cdc20, localize in centrosomes with pericentrin, and associate with γ-tubulin strongly suggests that it has a meiosis-specific role in centrosomes. However, it remains to be determined whether speriolin associates directly or indirectly with pericentrin and γ-tubulin in centrosomes.

We have confirmed that speriolin binds to testicular Cdc20 by pull-down assay. In addition, Cdc27 was recovered together with Cdc20 from testis lysate, suggesting that speriolin is in a complex with APC^{Cdc20}. From co-immunoprecipitation experiments, it is estimated that 10% of Cdc20 is co-precipitated with

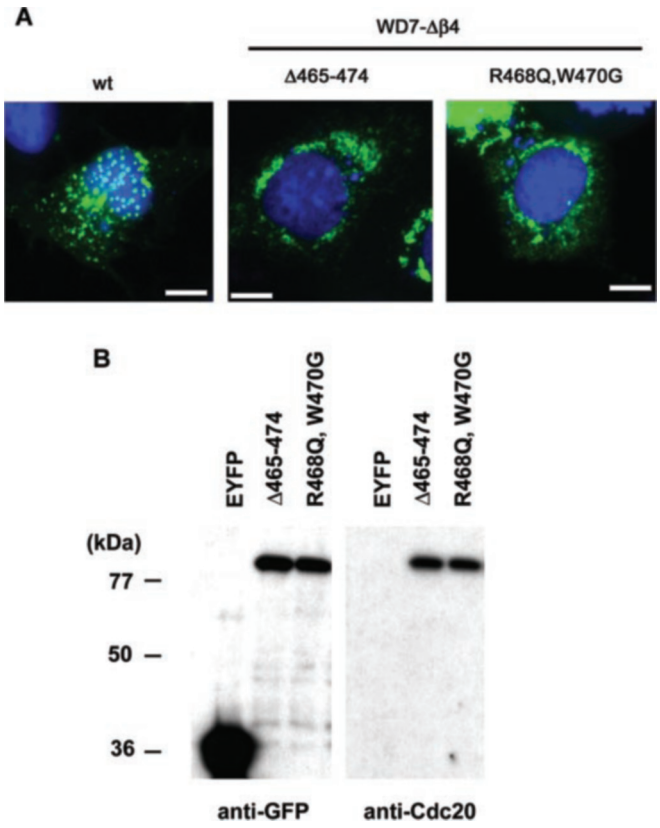

FIG. 10. **Accumulation of mutant Cdc20 in cytoplasm in COS-7 cells.** *A*, the last β strand of the C-terminal WD motif (WD7-β4; shown in Fig. 9) is indispensable for Cdc20 localization at the kinetochores. COS-7 cells were transiently transfected with EYFP-tagged wild type (*wt*) Cdc20 (*left panel*), a deletion mutant (Δ465–474), or a point mutant (R468Q and W470G) of Cdc20 that disrupts WD7-β4 (*WD7-Δβ4*). After 24 h, the transfected cells were observed by fluorescence microscopy. DNA was stained by DAPI. EYFP-Cdc20 was observed at the kinetochores but remained in the cytoplasm when WD7-β4 was disrupted (*right panels*). *Bar*, 10 μm. *B*, EYFP-tagged mutant versions of Cdc20 were expressed intact in COS-7 cells. Whole cell extracts were prepared from EYFP-Cdc20-expressing COS-7 cells and subjected to Western blotting using monoclonal antibodies to EYFP (anti-GFP) and Cdc20 (anti-Cdc20).

Mad2 (10) or APC (36) from mitotic HeLa cells or mitotic *Xenopus* egg extract, respectively. On the other hand, from our pull-down experiments, we estimate that 0.1% of testicular Cdc20 is recovered by GST-speriolin, as judged by Western blotting. However, the physical interaction between speriolin and Cdc20 during spermatogenesis is stage-specific and might occur in a Cdc20 structure-related manner. If speriolin selectively interacts with Cdc20 only when Cdc20 forms a β-propeller structure, the recovery of Cdc20 from testis lysates would be expected to be lower than that from synchronized mitotic cell extracts. It should be noted that speriolin is apparently present in an insoluble complex with APC^{Cdc20} in spermatogenic cells because speriolin and Cdc20 were detected in the 0.1% Nonidet P-40-insoluble fraction only in testis for the tissues examined.

Proteins that contain seven WD motifs are able to fold into a seven-blade β-propeller structure by interaction of the first β strand of the N-terminal WD motif (WD1-β1) and the last β strand of the C-terminal WD motif (WD7-β4) (37), and they assume an open relaxed form if either of these β strands is deleted (17, 18). It was shown recently that Cdc20 requires the Mad2/APC-interacting domain (amino acids 1–167) for localization to centrosomes and the N-terminal WD motif for localization to both centrosomes and kinetochores (6). We found that when glutamine and glycine were substituted for Arg-468 and Trp-470 in WD7-β4, Cdc20 was unable to bind speriolin or to enter the nucleus. These mutations also caused Cdc20 to form aggregates in the cytoplasm, similar to what was reported with disruption of folding of another seven-WD motif protein, the G protein β subunit (38). These results strongly suggest that Cdc20 needs to fold into a β-propeller structure to bind speriolin and to enter the nucleus and become available for association with kinetochores.

A hallmark of spermatogenesis is the expression of a substantial number of spermatogenic cell-specific genes that are either novel or orthologues of genes expression in somatic cells and have roles unique to spermatogenic cells (39, 40). In particular, there are meiosis-related proteins such as cyclin A1 (41), Rec8 (42, 43), and STAG3 (44) that supplant or complement similar proteins that function in mitosis. Whereas speriolin lacks homology with known Cdc20-binding or mitosis regulatory proteins that would provide clues about its function in meiosis, the results of these studies suggest some interesting possibilities for examination in future studies. One role of speriolin might be to regulate or stabilize the folding of Cdc20 by binding to WD7-β4. EYFP-Cdc20 failed to localize to the nucleus or to bind speriolin when this domain was deleted or its structure was disrupted by point mutations. Differences in the nuclear envelopes of spermatogenic and somatic cells might require the presence of speriolin for nuclear entry. These differences include the presence of spermatogenic cell-specific nuclear lamins (45–49) and the attachment of the synaptonemal complexes at both ends to the thick nuclear lamina lining the nuclear envelope of spermatocytes (50, 51). The present studies noted an increase in lamin B in the testis at day 18, coincident with the beginning of speriolin synthesis. In addition, the presence of Cdc20 during the postmeiotic phase of spermatogenesis might be attributable to it being bound by speriolin, thereby preventing it from being targeted to the APC. Gene targeting currently is being used to disrupt function of speriolin as an approach to determining its roles *in vivo* and following meiosis in spermatogenic cells.

Acknowledgments—We are grateful to Dr. Deborah O'Brien for helpful discussions, to Dr. Kiyoshi Miki for valuable technical advice, to Dr. Kiyoshi Miki and Dr. Bonnie Deroo for constructive comments on the manuscript, and to the other members of our laboratory for helpful discussions throughout the course of this work.

REFERENCES

1. Nigg, E. A. (2001) *Nat. Rev. Mol. Cell. Biol.* **2,** 21–32
2. Peters, J. M. (2002) *Mol. Cell* **9,** 931–943
3. Page, A. M., and Hieter, P. (1999) *Annu. Rev. Biochem.* **68,** 583–609
4. Weinstein, J. (1997) *J. Biol. Chem.* **272,** 28501–28511
5. Kallio, M., Weinstein, J., Daum, J. R., Burke, D. J., and Gorbsky, G. J. (1998) *J. Cell Biol.* **141,** 1393–1406
6. Kallio, M. J., Beardmore, V. A., Weinstein, J., and Gorbsky, G. J. (2002) *J. Cell Biol.* **158,** 841–847
7. Hwang, L. H., Lau, L. F., Smith, D. L., Mistrot, C. A., Hardwick, K. G., Hwang, E. S., Amon, A., and Murray, A. W. (1998) *Science* **279,** 1041–1044
8. Kim, S. H., Lin, D. P., Matsumoto, S., Kitazono, A., and Matsumoto, T. (1998) *Science* **279,** 1045–1047
9. Reimann, J. D., Freed, E., Hsu, J. Y., Kramer, E. R., Peters, J. M., and Jackson, P. K. (2001) *Cell* **105,** 645–655
10. Fang, G., Yu, H., and Kirschner, M. W. (1998) *Genes Dev.* **12,** 1871–1883
11. Reimann, J. D., Gardner, B. E., Margottin-Goguet, F., and Jackson, P. K. (2001) *Genes Dev.* **15,** 3278–3285
12. Taylor, S. S., and McKeon, F. (1997) *Cell* **89,** 727–735
13. Howell, B. J., McEwen, B. F., Canman, J. C., Hoffman, D. B., Farrar, E. M., Rieder, C. L., and Salmon, E. D. (2001) *J. Cell Biol.* **155,** 1159–1172
14. Lambright, D. G., Sondek, J., Bohm, A., Skiba, N. P., Hamm, H. E., and Sigler, P. B. (1996) *Nature* **379,** 311–319
15. Sondek, J., Bohm, A., Lambright, D. G., Hamm, H. E., and Sigler, P. B. (1996) *Nature* **379,** 369–374
16. Wall, M. A., Coleman, D. E., Lee, E., Iniguez-Lluhi, J. A., Posner, B. A., Gilman, A. G., and Sprang, S. R. (1995) *Cell* **83,** 1047–1058
17. Baker, S. C., Saunders, N. F., Willis, A. C., Ferguson, S. J., Hajdu, J., and Fülöp, V. (1997) *J. Mol. Biol.* **269,** 440–455
18. Neer, E. J., and Smith, T. F. (1996) *Cell* **84,** 175–178
19. Eaker, S, Pyle, A., Cobb, J., and Handel, M. A. (2001) *J. Cell Sci.* **114,** 2953–2965
20. Eaker, S, Cobb, J., Pyle, A., and Handel, M. A. (2002) *Dev. Biol.* **249,** 85–95
21. Wassmann, K., Niault, T., and Maro, B. (2003) *Curr. Biol.* **13,** 1596–1608
22. Woods, L. M., Hodges, C. A., Baart, E., Baker, S. M., Liskay, M., and Hunt,

P. A. (1999) *J. Cell Biol.* **145,** 1395–1406
23. Wu, G., Xu, G., Schulman, B. A., Jeffrey, P. D., Harper, J. W., and Pavletich, N. P. (2003) *Mol. Cell* **11,** 1445–1456
24. Guardavaccaro, D, Kudo, Y., Boulaire, J., Barchi, M., Busino, L., Donzelli, M., Margottin-Goguet, F., Jackson, P. K., Yamasaki, L., and Pagano, M. (2003) *Dev. Cell* **4,** 799–812
25. Margottin-Goguet, F., Hsu, J. Y., Loktev, A., Hsieh, H. M., Reimann, J. D., Jackson, P. K. (2003) *Dev. Cell* **4,** 813–826
26. Hassold, T., and Hunt, P. (2001) *Nat. Rev. Genet.* **2,** 280–291
27. Miki, K., and Eddy, E. M. (1998) *J. Biol. Chem.* **273,** 34384–34390
28. O'Brien, D. A. (1993) Methods Toxicol. **3A,** 246–264
29. Harper, J. W., Burton, J. L., and Solomon, M. J. (2002) *Genes Dev.* **16,** 2179–2206
30. Manandhar, G., Sutovsky, P., Joshi, H. C., Stearns, T., and Schatten, G. (1998) *Dev. Biol.* **203,** 424–434
31. Lin, M., Chang, J. K., Shankar, D., and Sakamoto, K. M. (2003) *Exp. Mol. Pathol.* **74,** 123–128
32. Gieffers, C., Peters, B. H., Kramer, E. R., Dotti, C. G., and Peters, J. M. (1999) *Proc. Natl. Acad. Sci. U. S. A.* **96,** 11317–11322
33. Zhang, Y., and Lees, E. (2001) *Mol. Cell. Biol.* **21,** 5190–5199
34. Kramer, E. R., Gieffers, C., Hölzl, G., Hengstschläger, M., and Peters, J. M. (1998) *Curr. Biol.* **8,** 1207–1210
35. Lorca, T., Castro, A., Martinez, A. M., Vigneron, S., Morin, N., Sigrist, S., Lehner, C., Doree, M., and Labbe, J. C. (1998) *EMBO J.* **17,** 3565–3575
36. Fang, G., Yu, H., and Kirschner, M. W. (1998) *Mol. Cell* **2,** 163–171
37. Vodermaier, H. C. (2001) *Curr. Biol.* **11,** R834–837
38. Garcia-Higuera, I., Fenoglio, J., Li, Y., Lewis, C., Panchenko, M. P., Reiner, O., Smith, T. F., and Neer, E. J. (1996) *Biochemistry* **35,** 13985–13994
39. Eddy, E. M. (1995) *Reprod. Fertil. Dev.* **7,** 695–704
40. Eddy, E. M., and O'Brien, D. A. (1998) *Curr. Top. Dev. Biol.* **37,** 141–200
41. Liu, D., Matzuk, M. M., Sung, W. K., Guo, Q., Wang, P., and Wolgemuth, D. J. (1998) *Nat. Genet.* **20,** 377–380
42. Parisi, S., McKay, M. J., Molnar, M., Thompson, M. A., van der Spek, P. J., van Drunen-Schoenmaker, E., Kanaar, R., Lehmann, E., Hoeijmakers, J. H., and Kohli, J. (1999) *Mol. Cell. Biol.* **19,** 3515–3528
43. Watanabe, Y., and Nurse, P. (1999) *Nature* **400,** 461–464
44. Prieto, I., Suja, J. A., Pezzi, N., Kremer, L., Martinez-A, C., Rufas, J. S., and Barbero, J. L. (2001) *Nat. Cell Biol.* **3,** 761–766
45. Alsheimer, M., and Benavente, R. (1996) *Exp. Cell Res.* **228,** 181–188
46. Furukawa, K., and Hotta, Y. (1993) *EMBO J.* **12,** 97–106
47. Furukawa, K., Inagaki, H., and Hotta, Y. (1994) *Exp. Cell Res.* **212,** 426–430
48. Smith, A., and Benavente, R. (1992) *Differentiation* **52,** 55–60
49. Vester, B., Smith, A., Krohne, G., and Benavente, R. (1993) *J. Cell Sci.* **104,** 557–563
50. Esponda, P., and Giménez-Martín, G. (1972) *Chromosoma* **38,** 405–417
51. Liebe, B., Alsheimer, M., Höög, C., Benavente, R., and Scherthan, H. (2003) *Mol. Biol. Cell* **15,** 827–837